REDVET - Revista electrónica de Veterinaria - ISSN 1695-7504
Vol 25, No. 1 (2024)
http://www.veterinaria.org
Article Received: 28/05/2024 Revised: 05/06/2024 Published:18/06/2024

Preparation Of Cadmium Doped Nanocrystalline Indium Oxide By Combustion Method And Its Gas Sensing Behaviour

Pawan M. Chatare[1*], Vivek D. Kapse[2], D. R. Patil[3]

[1]Mahatma Gandhi College of Science, Gadchandur, Tah- Korpana, Dist- Chandrapur
[2]Arts, Science and Commerce College, Chikhaladara, Dist- Amravati
[3]Bulk and Nanomaterials Research Laboratory, Department of Physics, R. L. College, Parola, Dist- Jalgaon

***Corresponding Author:** Pawan M. Chatare
*Email: pawanchatare@gmail.com

Abstract:
This work examines the combustion synthesis of cadmium (Cd) doped nanocrystalline indium oxide (In_2O_3) and its gas-sensing potential. This flexible n-type semiconductor, indium oxide has great potential for gas-sensing applications due to its high sensitivity and quick reaction to diverse gases. Strategic doping improves its performance. Cadmium doping was used to enhance gas-sensing capabilities in In_2O_3 by altering its structural, optical, and electrical characteristics. Combustion synthesis produces nanocrystalline materials with excellent purity and controllable shape quickly, cheaply, and scalable. Crystalline structure, shape, elemental content, and optical characteristics of produced Cd-doped In_2O_3 nanomaterials were confirmed using XRD, FESEM, EDX. The material's sensitivity, selectivity, and response-recovery to hydrogen, ammonia, and volatile organic molecules were tested in gas sensing tests. The study found that Cd doping improved gas-sensing capability in In_2O_3, including increased sensitivity, quicker reaction times, and reduced response times.

Keywords: Cadmium-doped indium oxide, Combustion synthesis, Nanocrystalline materials, Gas sensing, Semiconductor sensors

1. Introduction

The synthesis and gas sensing properties of Cd-doped In_2O_3 represent a cutting-edge area of research at the intersection of materials science, chemistry, and environmental sensing technology [1]. Indium oxide (In_2O_3), a well-known semiconductor material, has garnered significant attention due to its excellent optical and electrical properties, making it a promising candidate for a variety of applications, including gas sensors, transparent conductive electrodes, and photocatalysts. However, pure indium oxide often exhibits limitations in sensitivity, selectivity, and stability when employed as a gas-sensing material. To overcome these challenges, researchers have explored doping with various metal ions, such as cadmium (Cd), to tailor and enhance the material's physical and chemical properties. Cadmium doping introduces controlled defects and modifies the bandgap energy, leading to improved electrical conductivity, enhanced adsorption of gas molecules, and greater catalytic activity [2]. These modifications can significantly enhance the material's performance for detecting various gases, such as hydrogen, ammonia, or volatile organic compounds, which are critical for applications in environmental monitoring, industrial safety, and medical diagnostics. The synthesis process, whether via sol-gel, hydrothermal, or other techniques, plays a crucial role in determining the morphology, crystallinity, and surface area of the Cd-doped In_2O_3, which are key factors influencing its gas-sensing performance[3]. Additionally, understanding the interaction mechanisms between the doped material and target gas molecules is vital for optimizing sensor design and functionality. This research not only contributes to advancing the knowledge of functional oxide materials but also addresses the growing demand for highly sensitive, selective, and reliable gas sensors in modern technological applications.

2. Experimental

2.1. Materials and Synthesis

2.1.1 Materials

The principal raw materials included in this study were meticulously chosen according to their purity, particle size distribution and chemical reactivity. Indium nitrate hydrate ($In(NO_3)_3 \bullet xH_2O$, 99.99%) was obtained from Sigma-Aldrich and functioned as the principal precursor for the manufacture of indium oxide. The hydrated form was selected over the anhydrous variety because of its enhanced solubility properties and improved handling during the solution-based synthesis procedure [4]. For doping research high-purity metal salts namely cadmium nitrate tetrahydrate [$Cd(NO_3)_3 \cdot 4H_2O$] was employed. This dopant precursor was chosen for its compatibility with the synthesis method and its efficacy in integrating into the In_2O_3 crystal lattice without generating secondary phases. All chemical reagents were of analytical grade or superior and were utilized without further purification. The choice of these reagents was essential for attaining the intended nanostructure morphology and crystal phase purity. Citric acid monohydrate acted as the principal chelating agent, creating stable metal-citrate complexes that inhibited premature precipitation and guaranteed

REDVET - Revista electrónica de Veterinaria - ISSN 1695-7504
Vol 25, No. 1 (2024)
http://www.veterinaria.org
Article Received: 28/05/2024 Revised: 05/06/2024 Published:18/06/2024

uniform distribution of metal ions in the precursor solution. Ethylene glycol served as a polymerization agent, enabling the development of a polymer network that regulated particle growth during synthesis.

2.1.2 Synthesis process:
The synthesis of In_2O_3 nanostructures was accomplished through combustion method. The method was optimized to achieve specific morphological and structural characteristics of the final product [5].

2.1.2.1 Preparation of 1% Cadmium doped Indium oxide:
The preparation of cadmium-doped In_2O_3 involved three key steps: precursor solution preparation, combustion synthesis and calcinations [6]. In the first step i.e., preparation of the precursor solution**,** 1.96 g of indium nitrate and 0.031 g of cadmium nitrate (corresponding to a 1% doping concentration) were accurately weighed and dissolved in 50 ml of distilled water under continuous stirring to ensure homogeneity. Subsequently 2.5 g of urea was added to the solution acting as a fuel for the combustion reaction and stirred until it completely dissolved. In the second step the combustion synthesis began by transferring the prepared precursor solution to a glass beaker which was then placed on a hot plate. The solution was heated to 80°C under constant stirring to initiate the decomposition of urea. The temperature was maintained for 30 min allowing the urea to release gases, which led to an auto-ignition event and a rapid combustion reaction. This reaction resulted in the formation of a fluffy powder. Heating was continued for an additional 30 min to ensure complete combustion and the removal of residual organic components. In the final step, calcination, the synthesized powder was collected and transferred to a furnace. The powder was calcined at 500°C for 2 h to promote the crystallization of the Cd-doped In_2O_3 phase and enhance its structural integrity. This process ensured the production of a stable and well-crystallized material suitable for further characterization and gas-sensing applications.

2.1.2.2 Preparation of 3% and 5% Cadmium doped Indium oxide:
In the same way (as for preparation of 1% Cadmium doped Indium oxide) 3% and 5% Cadmium doped Indium oxide samples were prepared by varying the amount of cadmium nitrate and urea in the step 1 as per stoichiometric requirement.
For the preparation of 3% Cadmium doped Indium oxide 0.093 g of Cadmium nitrate (3% doping concentration) was used and the remaining procedure was exactly similar as for the preparation of 1% Cadmium doped Indium oxide.For the preparation of 5% Cadmium doped Indium oxide 0.155 g of Cadmium nitrate (5% doping concentration) was used and the remaining procedure was exactly similar as for the preparation of 1% Cadmium doped Indium oxide.

2.2 Material Characterization
The characterization of Cd-doped In_2O_3 utilized an extensive array of analytical methods to assess its structural, morphological and thermal characteristics [7]. Field Emission Scanning Electron Microscopy (FESEM) was utilized to examine the surface morphology of the produced Cd-doped In_2O_3. The investigation utilized a JEOL JSM-6390LV scanning electron microscope. Transmission Electron Microscopy (TEM) was employed to examine the internal structure and particle size of Cd-doped In_2O_3 at an elevated resolution utilizing a JEOL JEM-2100F TEM. Energy-dispersive X-ray spectroscopy (EDX or EDS) was employed for the elemental investigation and characterization of materials, including cadmium-doped indium oxide. Fourier Transform Infrared Spectroscopy (FTIR) was employed to analyze the functional groups and bonding in Cd-doped In_2O_3. The analysis utilized a PerkinElmer Spectrum 100 FTIR spectrometer. X-ray Diffraction (XRD) was employed to determine the phase identification and crystallinity of the Cd-doped In_2O_3 [8]. The investigation utilized a Rigaku Miniflex II diffractometer employing Cu Kα radiation. Gas sensing studies were performed utilizing a custom-designed sensor apparatus to assess the efficacy of Cd-doped In_2O_3 in identifying different target gases.

3. Results and Discussion
3.1 X-Ray Diffraction Analysis of Cadmium doped Indium Oxide
X-ray diffraction (XRD) analysis is essential for understanding the crystal structure, lattice parameters, crystallite size, and effects of cadmium (Cd) doping on indium oxide (In_2O_3). The X-ray diffraction (XRD) analysis of 1% cadmium (Cd) doped indium oxide (In_2O_3) reveals that the material predominantly retains the cubic bixbyite crystal structure characteristic of pure In_2O_3. The diffraction peaks observed at 2θ values of approximately 30.4°, 35.4°, and 50.9° correspond to the (2 2 2), (4 0 0) and (4 4 0) crystallographic planes, respectively (Figure 1). These peaks align closely with the standard JCPDS card (No. 06-0416) for indium oxide, confirming that the cubic phase is preserved even after doping with Cd [9]. A notable feature of the XRD pattern is the slight shift of the diffraction peaks to lower 2θ angles compared to pure In_2O_3. This shift is attributed to the substitution of Cd^{2+} ions (ionic radius ~0.97 Å) for In^{3+} ions (ionic radius ~0.80 Å) within the lattice. The larger size of Cd^{2+} causes lattice expansion, increasing the lattice parameter slightly. Additionally, this substitution introduces strain within the crystal lattice, leading to peak broadening. Overall, the XRD analysis confirms that Cd doping maintains the cubic structure of In_2O_3 while introducing lattice strain, peak shifts, and minor reductions in crystallinity and crystallite size [10]. These changes highlight the impact of Cd incorporation on the structural properties of indium oxide.

REDVET - Revista electrónica de Veterinaria - ISSN 1695-7504
Vol 25, No. 1 (2024)
http://www.veterinaria.org
Article Received: 28/05/2024 Revised: 05/06/2024 Published:18/06/2024

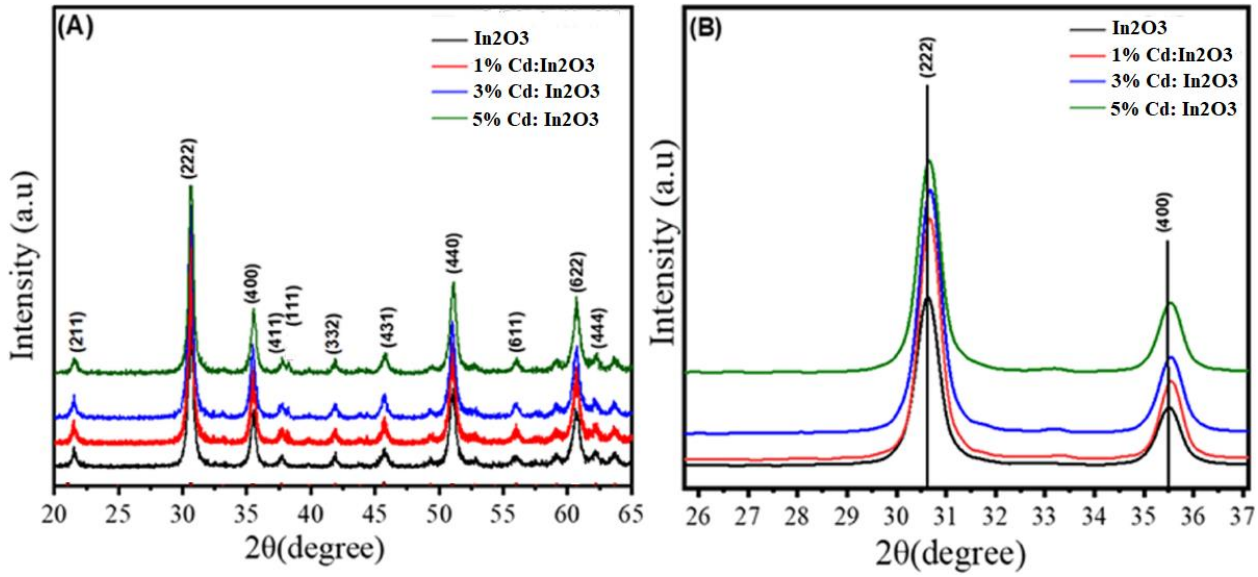

Figure 1: a) XRD spectra of 1%, 3% and 5% Cadmium doped Indium oxide., b) Enlarge view at peak position (2 2 2) & (4 0 0)

3.2 FTIR Spectral analysis of Cadmium doped Indium Oxide

In the present study comparative FTIR spectral analysis of 1%, 3%, and 5% cadmium (Cd) doped indium oxide ($In_2O_{3)}$ highlights the progressive changes in structural and surface.

Metal-Oxygen (M–O) Vibrations: The primary absorption bands observed in the 400–600 cm^{-1} range corresponding to the In–O stretching vibrations in the cubic bixbyite structure. FTIR spectra showed slight shifts to lower wavenumbers as the Cd doping level increases. This shift indicates lattice distortion caused by the substitution of Cd^{2+} ions (larger ionic radius) for In^{3+} ions. It was observed that band broadening is more pronounced at higher doping levels, reflecting increased lattice strain and defect formation (Figure 2).

O–H Vibrations: Absorption bands observed in the 3400–3500 cm^{-1} and 1600–1700 cm^{-1} ranges are attributed to O–H stretching and bending vibrations, associated with surface-adsorbed water or hydroxyl groups. A gradual reduction in the intensity of these bands is noted as Cd doping increases, suggesting that higher doping levels reduce surface hydroxylation (Figure 2).

Intensity Changes: It was observed in the spectra that the intensity of the metal-oxygen bands decreases slightly with increasing Cd doping, indicative of reduced crystallinity and possible disorder within the lattice [11].

Structural Modifications: The progressive shift and broadening of M–O bands observed and it confirmed lattice distortion caused by Cd incorporation, which increases with doping concentration.

Surface Changes: Reduced O–H band intensity was observed in the FTIR spectra suggests a decline in surface hydroxylation as doping increases, possibly due to changes in surface energy or chemical composition [12].

Crystallinity: Higher doping levels lead to decreased crystallinity and increased lattice strain, as evident from the changes in band intensity and broadening (Figure 2).

REDVET - Revista electrónica de Veterinaria - ISSN 1695-7504
Vol 25, No. 1 (2024)
http://www.veterinaria.org
Article Received: 28/05/2024 Revised: 05/06/2024 Published:18/06/2024

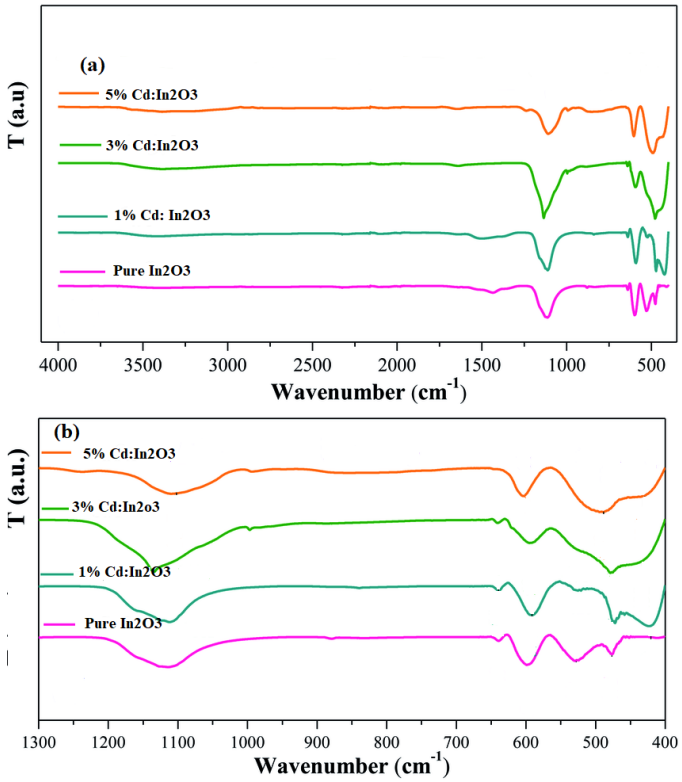

Figure 2: Comparative FTIR spectra of Pure In_2O_3, 1%, 3% & 5% Cd-doped In_2O_3.

3.3 Transmission Electron Microscopy (TEM) and Selected Area Electron Diffraction (SAED) analysis of Cadmium doped Indium Oxide

Particle Size

For 1% Cd-doped In_2O_3 small particle sizes, typically ranging from 5–10 nm indicating a less agglomerated structure were observed. Low doping concentration leads to minimal changes in lattice structure, preserving the intrinsic nanoparticle morphology. For 3% Cd-dopedIn_2O_3, slightly larger particle sizes around 10–15 nm due to increased cadmium incorporation was observed, which can promote particle growth and mild agglomeration. However, for 5% Cd:In_2O_3, noticeable particle growth with sizes reaching 15–20 nm was observed with more significant agglomeration (Figure 3).

Morphology

For 1% Cd:In_2O_3, uniform and spherical or slightly elliptical nanoparticles were observed. Low doping concentration maintains the original morphology of indium oxide. For 3% Cd:In_2O_3, particles observed to be more polyhedral or irregular due to lattice distortion caused by cadmium substitution. Moderate doping induces local strain, altering particle morphology. For 5% Cd-doped In_2O_3, significant morphological variation with some larger, elongated, or fused structures were observed. High doping levels lead to anisotropic growth and defect formation, disrupting uniform morphology.

Crystallinity

For 1% Cd-doped In_2O_3, high crystallinity with well-defined lattice fringes observed in TEM due to minimal lattice distortion from cadmium incorporation and for 3% Cd-doped In_2O_3 slightly reduced crystallinity with observable lattice distortion was observed. However, for 5% Cd-doped In_2O_3, significant reduction in crystallinity with more pronounced lattice distortions and defects was noticeable due to excess cadmium disrupts the indium oxide lattice, leading to defect-induced amorphization.

Lattice Spacing (d-spacing)

For 1% Cd-doped In_2O_3, Lattice fringes with a spacing close to pure In_2O_3, indicating minimal structural alteration. It is because; low doping does not significantly affect the lattice constants. For 3% Cd:In_2O_3, slight changes in d-spacing indicating successful cadmium incorporation. Cadmium ions slightly expand or contract the lattice depending on ionic radii differences. However, for 5% Cd:In_2O_3, significant variation in d-spacing, suggesting lattice distortion and defect formation because high doping levels lead to strain and disorder within the lattice.

REDVET - Revista electrónica de Veterinaria - ISSN 1695-7504
Vol 25, No. 1 (2024)
http://www.veterinaria.org
Article Received: 28/05/2024 Revised: 05/06/2024 Published:18/06/2024

Agglomeration
For 1% Cd-doped In_2O_3, low agglomeration with particles well-dispersed were observed because minimal doping reduces interparticle interaction. For 3% Cd-doped In_2O_3, moderate agglomeration was observed due to increased particle size and surface interaction. Higher doping enhances particle-particle interactions. However, for 5% Cd-doped In_2O_3, significant agglomeration with larger clusters was observed because excess cadmium promotes particle fusion and aggregation.

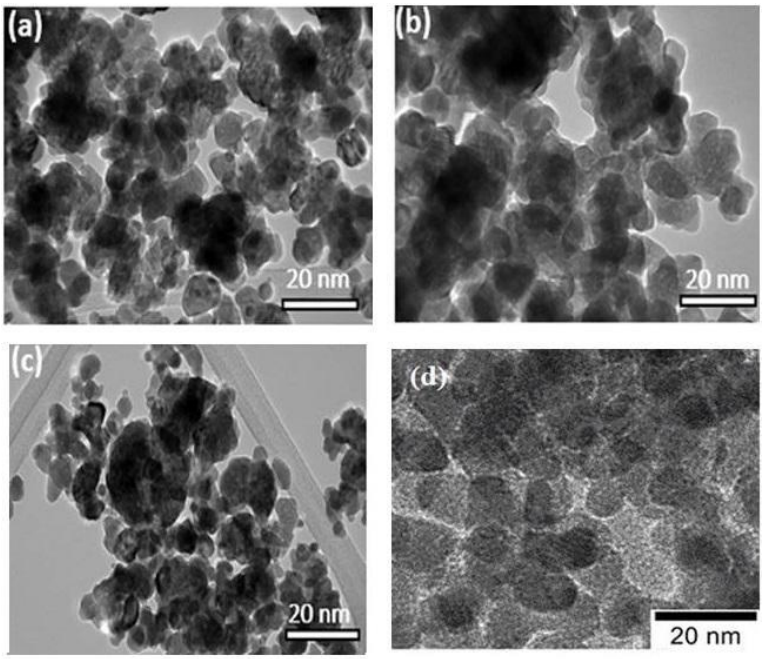

Figure 3: TEM images of (a)1% Cd-doped In_2O_3, (b) 3% Cd-doped In_2O_3, (c) 5% Cd-doped In_2O_3 and (d) Pure In_2O_3

3.4 Selected Area Electron Diffraction (SAED) analysis
Pure Indium Oxide
SAED Pattern: Sharp, bright and well-defined diffraction spots were observed indicative of a highly crystalline cubic bixbyite structure. Symmetry was found to be consistent with the body-centered cubic structure. Presence of indexed spots were observed corresponding to characteristic planes such as (2 1 1), (2 2 2), and (4 0 0).

1% Cadmium-Doped Indium Oxide
SAED Pattern: Similar to the pure indium oxide pattern with sharp diffraction spots. No significant distortion in the crystal lattice was noticed, suggesting that cadmium atoms substitute indium without disrupting the overall crystal structure. Slight changes in interplanar spacing were observed, indicating minor lattice strain due to the size difference between cadmium and indium ions [13].

3% Cadmium-Doped Indium Oxide
SAED Pattern: Sharp spots with some broadenings were observed. Slightly more pronounced lattice strain was noticed as cadmium concentration increases. No new phases detected, indicating cadmium atoms are still well-integrated into the indium oxide matrix.

5% Cadmium-Doped Indium Oxide
SAED Pattern: Diffraction spots start to show broadening and reduced intensity. Lattice strain appears to be more significant, potentially due to saturation of substitution sites or clustering of cadmium atoms.

Crystal Structure Stability: Pure indium oxide maintains its cubic bixbyite structure upon cadmium doping up to 3%. Higher doping levels (5%) introduced lattice distortions and secondary phases.

Lattice Strain: The gradual increase in lattice strain with doping is attributed to the ionic size difference between cadmium (Cd^{2+}) and indium (In^{3+}).

REDVET - Revista electrónica de Veterinaria - ISSN 1695-7504
Vol 25, No. 1 (2024)
http://www.veterinaria.org
Article Received: 28/05/2024 Revised: 05/06/2024 Published:18/06/2024

Crystallinity: High crystallinity is preserved in pure and lightly doped samples (1% and 3%). At 5% doping, crystallinity decreases, as evidenced by broadening and weakening of SAED spots.

Secondary Phases: At low doping levels (1% and 3%), cadmium atoms are effectively incorporated into the indium oxide matrix. At higher doping (5%), the presence of additional phases (e.g., CdO) observed due to limited solubility (Figure 4).
SAED analysis demonstrates that indium oxide retains its cubic crystal structure when doped with cadmium up to a threshold level. Increasing cadmium concentration introduces lattice strain, which is evident from the changes in diffraction patterns. Beyond 3% doping, the crystalline integrity diminishes, potentially leading to the formation of secondary phases [14].

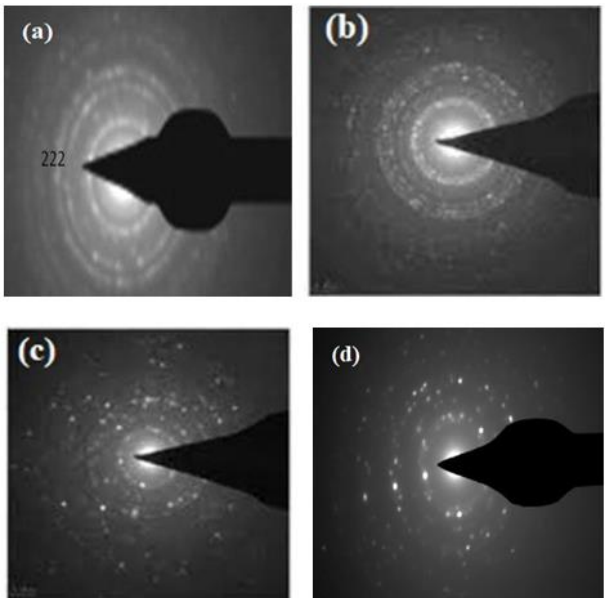

Figure 4 : Selected Area Electron Diffraction (SAED) images of (a) pure In_2O_3, (b)1% Cd-doped In_2O_3, (c) 3% Cd:In_2O_3 and (d) 5% Cd-doped In_2O_3.

3.5 Field Emission Scanning Electron Microscopy (FESEM) Analysis of Cadmium doped Indium Oxide
SEM analysis highlights the structural evolution of indium oxide with cadmium doping. While low Cd concentrations preserve surface integrity and grain uniformity, higher concentrations induce agglomeration and porosity which may affect the material's electronic and optical properties (Figure 5).

Grain Morphology: Pure indium oxide displayed uniformly shaped grains with minimal defects. It was observed that with increasing Cd doping, grain size decreases, and the surface becomes more irregular [15].

Agglomeration: Minimal agglomeration is observed in pure and 1% Cd-doped samples. Whereas noticeable clustering and porosity occur at higher doping levels (3% and 5%).

Porosity: It was observed that porosity increases with Cd doping, especially at 5%, likely due to lattice strain and structural reorganization.

Impact of Cadmium Doping: Low doping levels (1% and 3%) maintain better surface uniformity whereas excessive doping (5%) disrupts the morphology, reducing homogeneity and introducing defects.

REDVET - Revista electrónica de Veterinaria - ISSN 1695-7504
Vol 25, No. 1 (2024)
http://www.veterinaria.org
Article Received: 28/05/2024 Revised: 05/06/2024 Published:18/06/2024

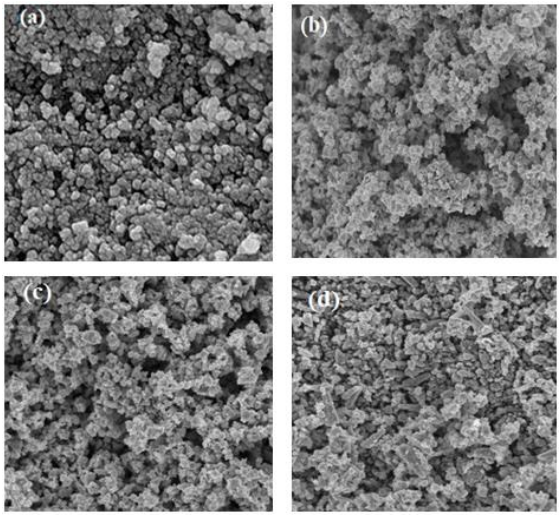

Figure 5: FESEM images of (a) pure In_2O_3, (b) 1% Cd:In_2O_3, (c) 3% Cd:In_2O_3 and (d) 5% Cd:In_2O_3.

3.6 EDS spectral analysis for Cadmium doped Indium oxide

Energy-dispersive X-ray spectroscopy (EDS) is used to analyze the elemental composition of materials. This analysis provides insight into the distribution and doping levels of cadmium in indium oxide samples. All samples showed strong In and O peaks, confirming the indium oxide base material. Cd peaks increase proportionally with the doping concentration. In pure indium oxide, the In:O ratio is consistent with stoichiometric In_2O_3. Cd:In ratio in doped samples closely matches the theoretical doping levels. At 1% and 3% doping cadmium is uniformly distributed throughout the sample. However, at 5% doping some regions may show Cd clustering suggesting a potential doping saturation limit. EDX spectra confirm the absence of unwanted impurities in all samples, ensuring high sample purity. EDX analysis verifies the successful incorporation of cadmium into the indium oxide matrix at doping levels of 1%, 3%, and 5%. While lower doping levels (1% and 3%) ensure uniform distribution, higher doping (5%) can lead to slight inhomogeneity or Cd clustering (Figure 6). This compositional analysis aligns well with the structural and morphological trends observed in SEM and SAED studies.

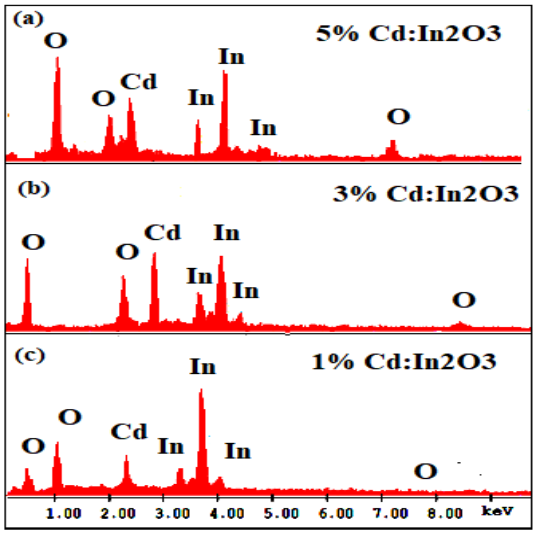

Figure 6: EDS image of (a) 5% Cd-doped In_2O_3, (b) 3% Cd-doped In_2O_3 and (c) 1% Cd-doped In_2O_3.

3.7 Gas sensing properties of Cadmium doped Indium oxide

Gas Response Analysis

The gas sensing response of cadmium-doped indium oxide for ethanol, LPG, CO_2, and NH_3 as target gases depends on the doping level (1%, 3%, and 5% Cd) and the specific interaction between the gas molecules and the doped oxide surface.

REDVET - Revista electrónica de Veterinaria - ISSN 1695-7504
Vol 25, No. 1 (2024)
http://www.veterinaria.org
Article Received: 28/05/2024 Revised: 05/06/2024 Published:18/06/2024

Ethanol (C_2H_6O) Gas Sensing

Ethanol molecules are oxidized on the sensor's surface, leading to a change in the resistance of In_2O_3. Cd doping can enhance sensitivity by increasing the number of active sites for adsorption.

For 1% Cd doping slight enhancement in sensitivity due to improved electron mobility and surface adsorption was observed. 3% Cd doping likely optimal doping as moderate Cd levels can enhance the chemisorption of ethanol molecules and hence increased sensitivity than 1% Cd doping was observed. For 5% Cd doping possible saturation or decline in sensitivity was observed due to excessive doping, which can introduce defects that reduce electron mobility.

Liquefied Petroleum Gas (LPG)

LPG molecules (mainly propane and butane) interact weakly with the surface requiring high temperatures for oxidation and detection. For 1% Cd doping minor improvement in response was observed therefore it can be concluded that low doping levels might not significantly alter the adsorption behavior. 3% Cd doping showed enhanced sensitivity due to increased surface oxygen vacancies facilitating LPG oxidation. For 5% Cd doping reduced response compared to 3% was observed which can be attributed to defect clustering which could reduce active sites.

Carbon Dioxide (CO_2)

For 1% Cd doping limited response was observed because CO_2 adsorption remains weak. 3% Cd showed slight enhancement in sensitivity because doping improves oxygen vacancy formation, increasing adsorption capacity. For 5% Cd doping insignificant improvement or reduced response was observed due to defect saturation and poor interaction of CO_2 with the surface.

Ammonia (NH_3)

NH_3 donates electrons to the In_2O_3 surface, reducing the resistance of the sensor. Doping affects the interaction strength and adsorption sites.For 1% Cd doping improved sensitivity was observed due to enhanced surface reactivity. 3% Cd doping showed optimal response due to increased interaction sites and adsorption capacity. For 5% Cd doping decrease in sensitivity compared to 3% was observed due to excessive doping, which may block active sites or reduce conductivity.

4. Gas Response of Cd-doped In_2O_3

Figure 7 represents the variation of gas response with temperature for Cd-doped In_2O_3 towards ethanol (100 ppm) at 375 K. The gas response of Cd-doped In_2O_3 shows a significant enhancement compared to pure In_2O_3, with increasing Cd concentration leading to improved sensitivity. The response rises with temperature, reaching a peak around 375 K before declining due to reduced gas adsorption at higher temperatures. Among the samples, 3% Cd-doped In_2O_3 exhibits the highest response (4.7) towards ethanol (100 ppm) gas at 375 K, closely followed by 5% Cd-doped In_2O_3, indicating that Cd doping enhances the sensing properties by modifying the electronic structure and increasing oxygen vacancies. Pure In_2O_3 demonstrates the lowest response across all temperatures, confirming the beneficial role of Cd in improving gas detection. The findings suggest that 3% Cd-doped In_2O_3 is the most effective composition, operating optimally at approximately 375 K, making it a promising material for gas sensor applications.

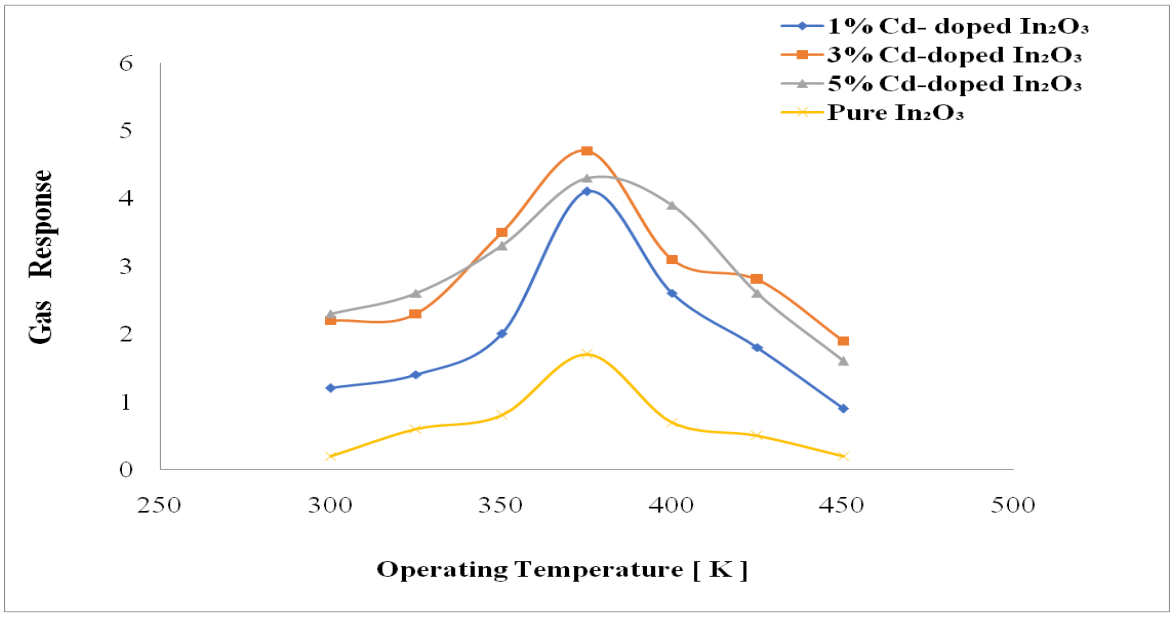

Figure 7: Graph of gas response versus temperature (K) for Cd-doped In_2O_3.

REDVET - Revista electrónica de Veterinaria - ISSN 1695-7504
Vol 25, No. 1 (2024)
http://www.veterinaria.org
Article Received: 28/05/2024 Revised: 05/06/2024 Published:18/06/2024

5. Selectivity of Cd-doped In_2O_3

The selectivity analysis of Cd-doped In_2O_3 based on the provided graph reveals that the material exhibits the highest response toward ethanol across all doping concentrations, indicating its strong selectivity for ethanol detection. Among the Cd-doped samples, 3% Cd-doped In_2O_3 demonstrates the highest response (4.7) towards ethanol gas at 375 K, suggesting that this composition is the most effective for ethanol sensing. The response to other gases, including LPG, CO_2 and NH_3 is comparatively lower, with LPG and NH_3 showing moderate responses and CO_2 having the lowest overall sensitivity. Pure In_2O_3 exhibits significantly lower responses for all gases, confirming that Cd doping enhances both sensitivity and selectivity. Overall, Cd-doped In_2O_3 is most selective for ethanol, making it a promising material for ethanol gas sensing applications, with 3% Cd doping showing the best performance in terms of both response and selectivity. Figure 8 depicts the selectivity of the Cd-doped In_2O_3 thick film for Ethanol (100 ppm) at 375 K.

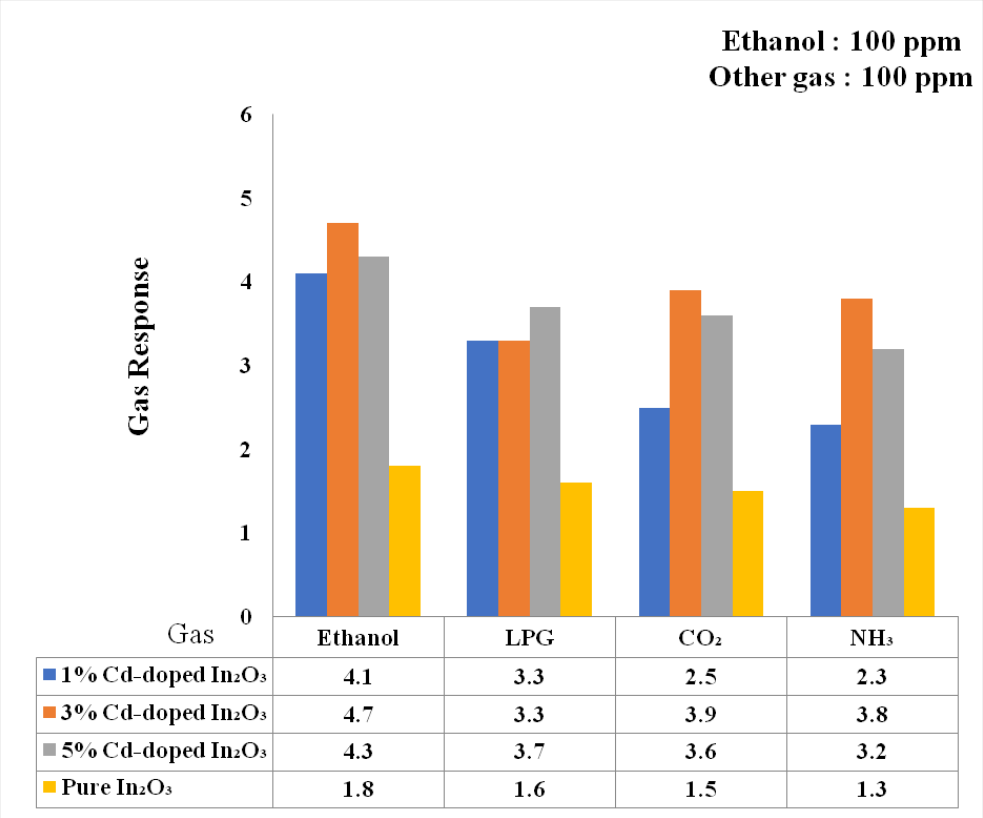

Gas	Ethanol	LPG	CO_2	NH_3
1% Cd-doped In_2O_3	4.1	3.3	2.5	2.3
3% Cd-doped In_2O_3	4.7	3.3	3.9	3.8
5% Cd-doped In_2O_3	4.3	3.7	3.6	3.2
Pure In_2O_3	1.8	1.6	1.5	1.3

Figure 8 : Selectivity of the Cd-doped In_2O_3 thick film for Ethanol (100 ppm) at 375 K.

6. Gas Response vs. Ethanol Concentration

The graph in figure 9 illustrates the relationship between gas response ($S = R_{air} / R_{gas}$) and ethanol concentration (20–160 ppm). At lower concentrations (20–60 ppm), the response increases gradually, indicating minimal sensitivity in this range. A significant rise occurs around 80 ppm, with a sharp increase observed, where the response reaches 4.7 towards ethanol (100 ppm) at 375 K. Beyond this, the response steeply rises, peaking at 4.8 at 160 ppm. The trend suggests that the sensor exhibits higher sensitivity between 100–1600 ppm, with saturation effects appearing beyond 140 ppm. This behaviour highlights the sensor's optimal ethanol detection range, particularly for concentrations above 100 ppm .

REDVET - Revista electrónica de Veterinaria - ISSN 1695-7504
Vol 25, No. 1 (2024)
http://www.veterinaria.org
Article Received: 28/05/2024 Revised: 05/06/2024 Published:18/06/2024

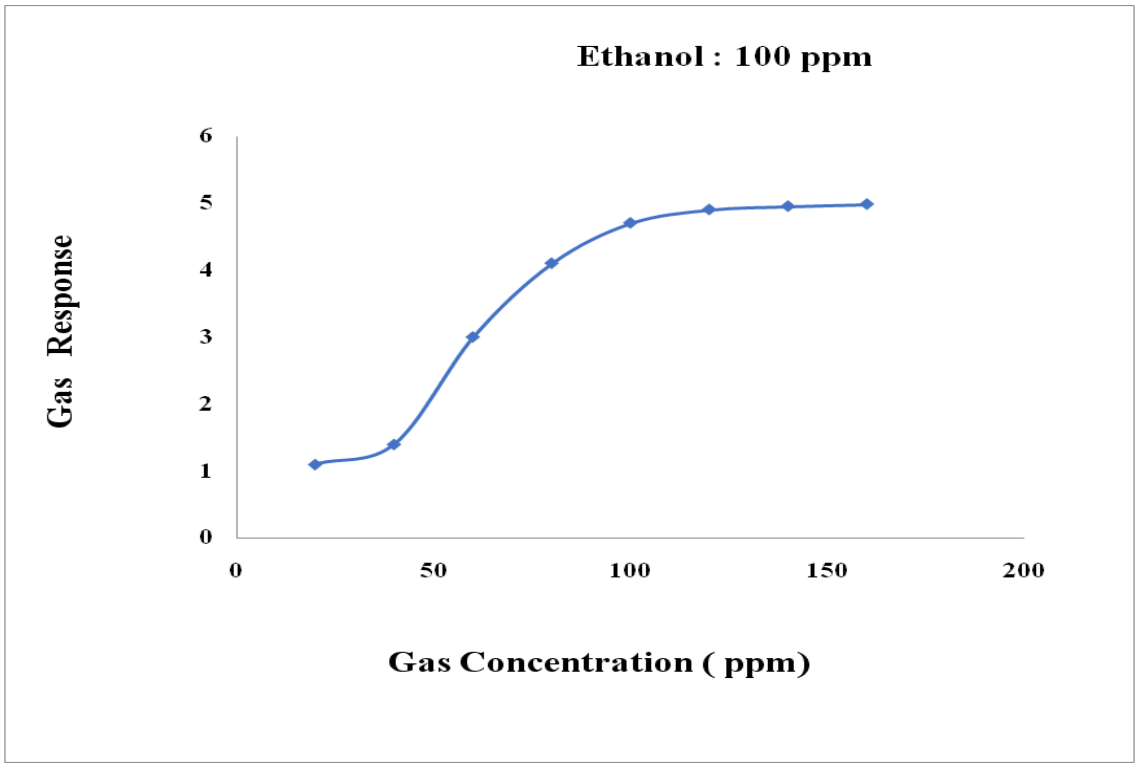

Figure 9 : Variation of ethanol gas versus concentration for 3% Cd-doped In_2O_3 at 375K.

7. Response-Recovery Characteristics

Figure 10 depicts the variation of gas response over time, with the x-axis representing time (sec) and the y-axis showing gas response values (0–6). Initially, the response is near zero, indicating no significant interaction. Around the 40 sec mark, a steep rise is observed, suggesting active gas detection and interaction with the sensor. The response peaks slightly above 4.5, stabilizing for a period, indicating a steady interaction phase stated as response time (10 sec) towards ethanol (100 ppm). After approximately (80 sec), the response begins to decline, suggesting gas desorption or concentration reduction. By 140 sec, it approaches baseline levels, indicating complete gas recovery time is (40 sec). This characteristic curve reflects a typical gas sensor response, comprising adsorption, peak detection, and desorption phases.

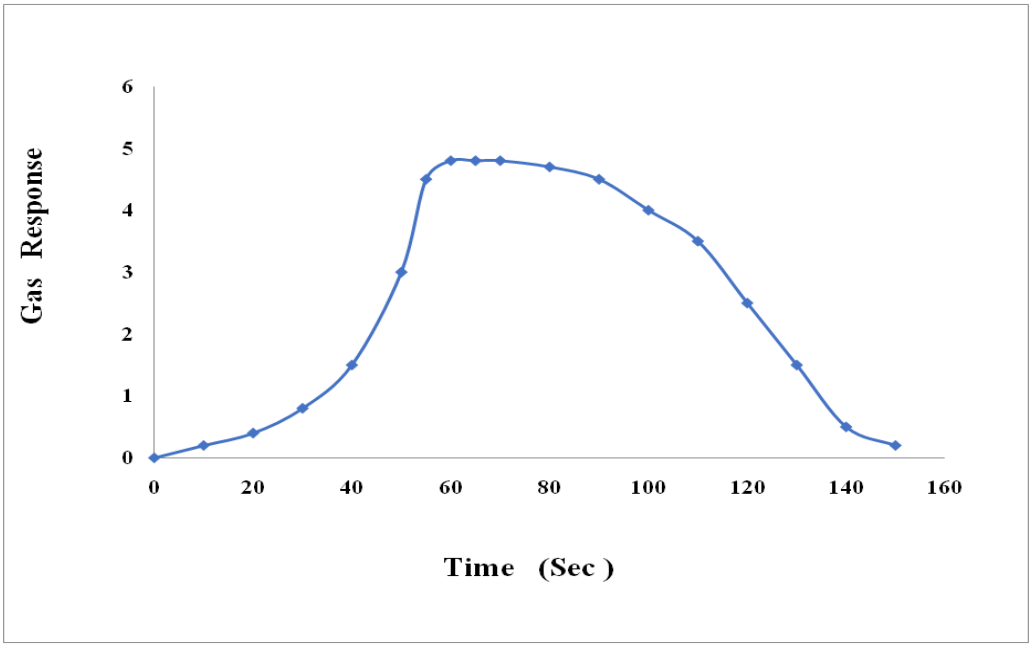

Figure 10 : Transient response characteristics of 3% Cadmium doped indium oxide to 100 ppm ethanol gas at 375K.

REDVET - Revista electrónica de Veterinaria - ISSN 1695-7504
Vol 25, No. 1 (2024)
http://www.veterinaria.org
Article Received: 28/05/2024 Revised: 05/06/2024 Published:18/06/2024

8. Stability

Figure 11 illustrates the relationship between gas response and time over a 90-day period at interval of 10 days. The response remains consistently stable at 4.7 towards ethanol (100 ppm) at 375 K throughout, with no observable fluctuations. This indicates that the system is in a steady state, with environmental or experimental conditions remaining unchanged. Such stability suggests that the sensor has reached equilibrium or is unaffected by external influences over time. This trend highlights the sensor's reliability and consistency, demonstrating its sustained performance over an extended period .

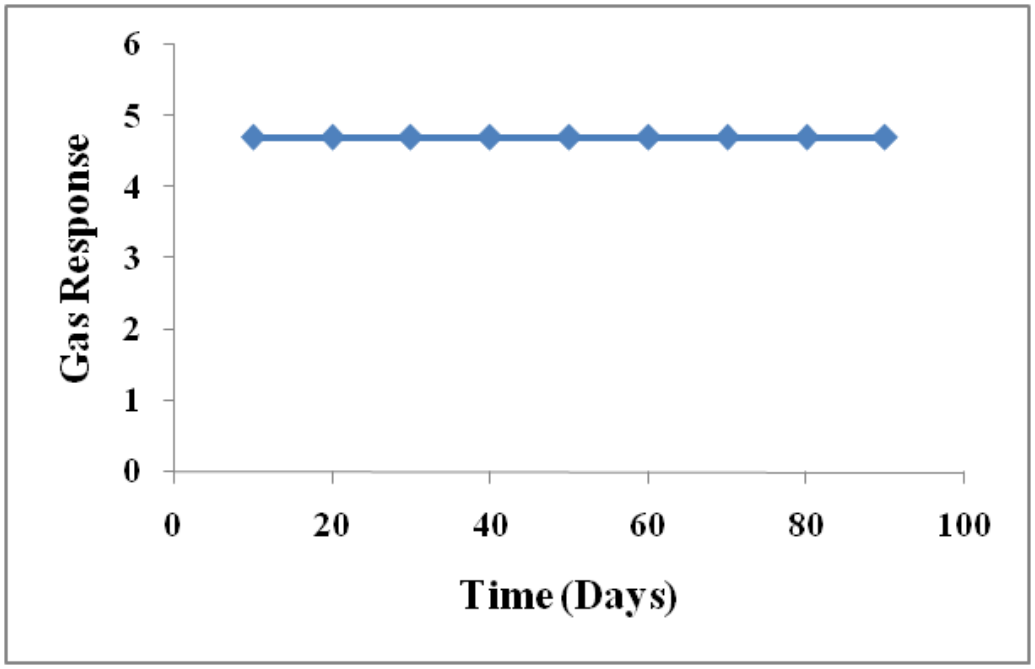

Figure 11: Stability of 3% Cd-doped In_2O_3.

The gas sensing performance of Cd-doped In_2O_3 varies depending on the doping concentration (1%, 3%, and 5%) and the interaction between gas molecules and the sensor surface. 3% Cd-doped In_2O_3 exhibits the highest response (4.7) towards ethanol (100 ppm) at 375 K, due to enhanced chemisorption and active site availability, while excessive doping at 5% reduces sensitivity due to defect saturation. Ethanol sensing improves with moderate doping (3%) but declines at higher levels due to defect clustering. Carbon dioxide shows minimal response across all doping levels, with slight improvement at 3% Cd due to increased oxygen vacancies. Ammonia sensing follows a similar trend, with optimal response at 3% doping and reduced sensitivity at 5% due to blocked adsorption sites. The sensor's response to ethanol is highly selective, with stable performance over time, making it a promising material for ethanol detection applications.

9. Conclusion:

The preparation of cadmium-doped nanocrystalline indium oxide via the combustion synthesis method has demonstrated its potential as a highly effective material for gas-sensing applications. The strategic incorporation of cadmium as a dopant significantly enhanced the structural, optical and electrical properties of the base material making it more sensitive and selective towards various target gases.3% Cadmium doped indium oxide highest response and sensitivity towards ethanol gas. The combustion method proved to be a cost-effective and efficient approach for producing high-purity nanocrystalline materials with controlled morphology and uniform dopant distribution. The synthesized Cd-doped In_2O_3 exhibited promising gas-sensing behavior characterized by improved sensitivity, faster response and recovery times for particularly 3% Cadmium doped indium oxide sensor towards the ethanol gas. These attributes make Cd-doped In_2O_3 an excellent candidate for environmental monitoring, industrial safety and medical diagnostics. This research highlights the importance of material design and synthesis techniques in advancing gas sensor technology and opens avenues for further optimization and exploration of doped metal oxides for next-generation sensing devices.

Reference

1. Yu, C.-W., Fu, H.-W., Yang, S.-M., Lin, Y.-S., & Lu, K.-C. (2023). Controlled Synthesis and Enhanced Gas Sensing Performance of Zinc-Doped Indium Oxide Nanowires. Nanomaterials, 13(7), 1170. https://doi.org/10.3390/nano13071170

2. Sen, P., Bhattacharya, P., Mukherjee, G., Ganguly, J., Marik, B., Thapliyal, D., Verma, S., Verros, G. D., Chauhan, M. S., & Arya, R. K. (2023). Advancements in Doping Strategies for Enhanced Photocatalysts and Adsorbents in Environmental Remediation. Technologies, 11(5), 144. https://doi.org/10.3390/technologies11050144
3. Kumarage, G. W. C., Hakkoum, H., & Comini, E. (2023). Recent Advancements in TiO_2 Nanostructures: Sustainable Synthesis and Gas Sensing. Nanomaterials, 13(8), 1424. https://doi.org/10.3390/nano13081424
4. Chiang, J.-L., Yadlapalli, B. K., Chen, M.-I., & Wuu, D.-S. (2022). A Review on Gallium Oxide Materials from Solution Processes. Nanomaterials, 12(20), 3601. https://doi.org/10.3390/nano12203601
5. Kurmashov, P. B., Ukhina, A. V., Manakhov, A., Ishchenko, A. V., Maksimovskii, E. A., & Bannov, A. G. (2023). Solution Combustion Synthesis of Ni/Al_2O_3 Catalyst for Methane Decomposition: Effect of Fuel. Applied Sciences, 13(6), 3962. https://doi.org/10.3390/app13063962
6. Ghasempour, A., Dehghan, H., Ataee, M., Chen, B., Zhao, Z., Sedighi, M., Guo, X., & Shahbazi, M.-A. (2023). Cadmium Sulfide Nanoparticles: Preparation, Characterization, and Biomedical Applications. Molecules, 28(9), 3857. https://doi.org/10.3390/molecules28093857
7. Ranjan, Rajeev & Mohan, Chandra &Choubey, s.K. & Tiwary, Kamala. (2023). Study of structural, morphological and optical properties of Mn+2 doped CdS nanoparticles synthesized at various doping concentration. Chalcogenide Letters. 20. 709-724. 10.15251/CL.2023.2010.709.
8. Ali, A., Chiang, Y. W., & Santos, R. M. (2022). X-ray Diffraction Techniques for Mineral Characterization: A Review for Engineers of the Fundamentals, Applications, and Research Directions. Minerals, 12(2), 205. https://doi.org/10.3390/min12020205
9. Saravanakumar Karunamoorthy, Jagan Govindan, Lee Jongh, Park Chang Min. (2023). MOF-derived C, N-In2O3 with GdFeO3 Z-scheme heterostructure for the photocatalytic removal of tetracycline, 2059-7037, https://doi.org/10.1038/s41545-023-00288-0.
10. S.K. Jasmin Vijitha, K. Mohanraj, R.P. Jebin,Structural, optical, and surface modifications by varying precursor concentrations on spray deposition of In doped Co3O4 thin films for electro chemical application, Chemical Physics Impact, Volume 6, 2023, 100143, ISSN 2667-0224,https://doi.org/10.1016/j.chphi.2022.100143.
11. Omar Muktaridha, Muhammad Adlim, SuhendrayatnaSuhendrayatna, Ismail Ismail,Progress of 3d metal-doped zinc oxide nanoparticles and the photocatalytic properties,Arabian Journal of Chemistry,Volume 14, Issue 6,2021,103175,ISSN 1878-5352,https://doi.org/10.1016/j.arabjc.2021.103175.
12. Hamrouni, A., Moussa, M., Fessi, N., Palmisano, L., Ceccato, R., Rayes, A., & Parrino, F. (2023). Solar Photocatalytic Activity of Ba-Doped ZnO Nanoparticles: The Role of SurfaceHydrophilicity. *Nanomaterials*, *13*(20),2742. https://doi.org/10.3390/nano13202742
13. Bertolotti, Federica, Nedelcu, Georgian, Vivani, Anna, Cervellino, Antonio, Masciocchi, Norberto, Guagliardi, Antonietta,Kovalenko, Maksym V. (2019), American Chemical Society ,Volume 13, Issue 12, ISSN 1936-0851, https://doi.org/10.1021/acsnano.9b07626
14. Norton, K. J., Alam, F., & Lewis, D. J. (2021). A Review of the Synthesis, Properties, and Applications of Bulk and Two-Dimensional Tin (II) Sulfide (SnS). *Applied Sciences*, *11*(5), 2062. https://doi.org/10.3390/app11052062
15. Karmaoui, Mohamed,Jorge, Ana Belen,McMillan, Paul F.,Aliev, Abil E.,Pullar, Robert C.,Labrincha, JoãoAntónio,Tobaldi, David Maria, (2018),American Chemical Society,volume 3, Issue 10,https://doi.org/10.1021/acsomega.8b02122